Tikrit Journal of Engineering Sciences (2024); 31(1): 161-171
DOI: http://doi.org/10.25130/tjes.31.1.14

IRAQI Academic Scientific Journals

ISSN: 1813-162X (Print); 2312-7589 (Online)
Tikrit Journal of Engineering Sciences
available online at: http://www.tj-es.com

TJES Tikrit Journal of Engineering Sciences

Climate Change's Impacts on Drought in Upper Zab Basin, Iraq: A Case Study

Doaa R. Mohammed *, Ruqayah K. Mohammed
Department of Civil Engineering, University of Babylon, Hilla, Iraq.

Keywords:
Drought Severity; Climate Change; LARS-WG Model; RDI Index; Upper Zab Basin.

Highlights:

- *Iraq, with its semiarid and desert climate, is expected to be highly affected by the impacts of global warming.*
- *The estimation of future climate throughout this century considered the RCP4.5 and RCP8.5 emission scenarios.*
- *Validation of the model involved thirty years of historical data against climate data from the Upper Zab Basin (1990–2021). Presented the effects of the Separation zone on the system.*
- *Precipitation projections from the GCMs exhibited diverse patterns, indicating significant uncertainty.*
- *During the 1999–2000 and 2007–2008 droughts, the downstream sub-basin experienced more severe conditions, with average RDIst values of -1.97 and -1.64, respectively.*

ARTICLE INFO
Article history:

Received	08 July	2023
Received in revised form	13 Sep.	2023
Accepted	30 Sep.	2023
Final Proofreading	25 Nov.	2023
Available online	22 Feb.	2024

Citation: Mohammed DR, Mohammed RK. **Climate Change's Impacts on Drought in Upper Zab Basin, Iraq: A Case Study**. *Tikrit Journal of Engineering Sciences* 2024; **31**(1): 161-171.
http://doi.org/10.25130/tjes.31.1.14

**Corresponding author:*
Doaa R. Mohammed
Department of Civil Engineering, University of Babylon, Hilla, Iraq.

Abstract: Iraq has a semiarid and desert climate. Also, it is predicted to be more susceptible to global warming effects. In the present study, daily climatic data from the past and projected future of the Upper Zab Basin, located in northern Iraq and considered an example of arid and semiarid climate conditions, were simulated using LARS-WG 6.0, i.e., a stochastic weather generator. The model also estimated daily rainfall and temperature. Using the RCP4.5 and RCP8.5 main emission scenarios, the future climate throughout the current century was estimated utilizing the MIROC5, CanESM2, HadGEM2-ES, ESM1-M, and CSIRO-Mk3.6.0 general circulation models (GCMs). This estimation was performed considering the significant uncertainty of future climate estimates. The model, constructed using thirty years' worth of historical data, was validated using climate data from the Upper Zab Basin in northern Iraq (1990–2021). According to the data, the average monthly maximum temperature will decline by 2.15–6.20 °C under RCP4.5 and 1.81–6.10 °C under RCP8.5 by the end of the twenty-first era for the corresponding upstream and downstream sub-basins. Precipitation projections from all GCMs showed varying patterns. Given that some models, like CanESM2, expected a rise in precipitation, while others, like MIROC5, forecasted a future with no change in precipitation or a falling trend, which illustrates the significant level of uncertainty in precipitation forecast when only one model was utilized. Also, the downstream sub-basin suffered the most during the 1999–2000 and 2007–2008 droughts, with average RDI_{st} values of -1.97 and -1.64, respectively. However, the upstream sub-basin had moderate to severe droughts in 1999–2000 and 2007–2008, with average RDI_{st} values of -0.81 and -1.84, respectively. The water available in the research location will be significantly impacted by variations in rainfall and temperature.

آثار تغير المناخ على الجفاف في حوض الزاب الأعلى، العراق: دراسة حالة

دعاء رياض محمدعلي، رقية كاظم محمد

قسم الهندسة المدنية / كلية الهندسة / جامعة بابل / الحلة – العراق.

الخلاصة

يمتلك العراق مناخ جاف وشبه جاف ومن المتوقع أن يكون أكثر عرضة لتأثيرات الاحتباس الحراري. في الدراسة الحالية، تمت محاكاة البيانات المناخية اليومية من الماضي والمستقبل باستخدام برنامج لارس LARS-WG 6.0، وهو مولد طقس عشوائي. تم استخدام النموذج أيضًا لتقدير هطول الأمطار اليومي ودرجة حرارة اليوم. استخدام سيناريوهات الانبعاث الرئيسية RCP4.5 و RCP8.5 لتقدير المناخ المستقبلي على مدار القرن الحالي باستخدام خمس نماذج للاحتباس الحراري العامة وهي كالتالي MIROC5 و CanESM2 و HadGEM2-ES و ESM1-M و CSIRO-Mk3.6.0 وذلك لمناقشة عدم اليقين الناتج من هذه الموديلات. تم التحقق من صحة النموذج، الذي تم إنشاؤه باستخدام بيانات تاريخية لمدة ثلاثين عامًا، باستخدام بيانات مناخية من حوض الزاب الأعلى والتي تقع في شمال العراق وتعتبر نموذجاً للظروف المناخية القاحلة وشبه القاحلة، للفترة (١٩٩٠-٢٠٢١). وفقًا للبيانات، ستنخفض درجة الحرارة القصوى الشهرية من ٢,١٥ – ٦,٢٠ درجة مئوية وفقا للسيناريو RCP4.5 و١,٨١–٦,١٠ درجة مئوية وفقا للسيناريو RCP8.5، بحلول نهاية القرن الحادية والعشرين. اظهرت توقعات هطول الأمطار من جميع نماذج الاحتباس الحراري أنماطًا متفاوتة. حيث أن بعض النماذج، مثل CanESM2، تتوقع ارتفاعًا في هطول الأمطار بينما لا تتوقع نماذج أخرى، مثل MIROC5، اي تغيير في هطول الأمطار، مما يوضح المستوى الكبير من عدم اليقين في التنبؤ بهطول الأمطار عند استخدام نموذج واحد فقط. علاوة على ذلك، عانى الحوض الفرعي عند المصب أكثر من غيره خلال فترات الجفاف في الفترة ١٩٩٩-٢٠٠٠ و٢٠٠٧-٢٠٠٨، حيث بلغ متوسط قيم RDI_{st} -1.97 و-١,٦٤ على التوالي. ومع ذلك، فقد تعرض الحوض الفرعي عند المنبع لموجات جفاف معتدلة إلى شديدة في الفترتين ١٩٩٩-٢٠٠٠ و٢٠٠٧-٢٠٠٨، حيث بلغ متوسط قيم RDI_{st} -0.81 و-١,٨٤، على التوالي. ستتأثر كمية المياه المتوفرة في موقع البحث بشكل كبير بالتغيرات في هطول الأمطار ودرجة الحرارة.

الكلمات الدالة: شدة الجفاف؛ تغير المناخ؛ نموذج LARS-WG؛ مؤشر RDI؛ حوض الزاب الأعلى.

1.INTRODUCTION

The Intergovernmental Panel on Climate Change reports a change in the climate (IPCC), which is currently one of the world's most prominent ecological issues (AR5). Due to global warming, numerous areas have experienced variations in rainfall, temperature, regularity of rainstorms, sea level, and air quality [1]. At the end of the 21st century, temperatures are anticipated to rise from 2.6 to 4.8 °C, according to the AR5, while variations in precipitation throughout the globe will affect effective rainfall and the amount of water that is readily available [2]. In some dry or desert places, there will be a reduction in runoff of between 10% and 30% due to the anticipated decrease in precipitation and greater amounts of evaporation. All representative concentration pathways (RCPs) predict that global warming will persist this century due to rising GHG (greenhouse gas emissions) caused by anthropogenic activities, the burning of fossil fuels, and changes in land usage [1, 3]. Due to its dry and semiarid climate, the Middle East is one of the most affected areas by global climate change. Water shortages would come from a significant rise in temperatures combined with a decrease in rainfall. Iraq is among the nations in the region that are most at risk from climate change [3]. Consequently, it will have to deal with environmental problems, such as a decline in readily available water and a growth in the population; therefore, the demand for water and the temperature rise. Increased extreme occurrences that harm the environment due to downscaling approaches will worsen this. Another downscaling method represented the complicated interaction between local surface variables (also known as predictands) and large-scale atmospheric variables (also known as predictors) using the "stepwise cluster analysis method" and the statistical downscaling tool SCADS [1]. Furthermore, high-resolution climate forecasts are produced using the regional modeling system Producing Regional Climates for Impacts Studies (PRECIS) to determine the local-scale impacts of anticipated climatic changes [1]. Numerous scholars have examined the effects of climate change on arid and semiarid climates, [1, 3, 7, 11, 16, 17] most did not consider the projection of weather variables to evaluate the meteorological drought. Mohammed and Hassan [1] and Khalaf et al. [11] predicted future changes in the climate of the southern region of Iraq using five global climate models (GCMs): CSIRO-Mk3.6.0, HadGEM2-ES, CanESM2, MIROC5, and NorESM1-M, based on two emission scenarios: RCP8.5 and RCP4.5, during three selected periods: 2021–2040, 2051–2070, and 208–1100. Mohammed and Scholz [7] used the UZRB as an example basin to illustrate how dry and semiarid climate conditions might affect long-term fluctuations and distributions of meteorological data on regional drought and aridity over the previous 35 years (1979-2014). Agha [16] examined the drought in the Nineveh region using the Chinese Z index for a one-month time frame. For the Mosul, Sinjar, and Tal Afar stations, historical data from 1981 to 2018 were used. Awchi and Jasim [17] examined and assessed Iraq's metrological draught. Twenty-two meteorological stations dispersed around Iraq were used to gather data on monthly rainfall from 1970 to 2010. The data accuracy was examined using several statistical methods, including the homogeneity test, trend analysis, and consistency test. Two tools were

used to examine the metrological draught and assess its properties: the Standard Precipitation Index (SPI) and the Theory of Runs. Statistical downscaling methods were utilized in this study instead of dynamic downscaling methods since they are more straightforward to apply, use fewer computer resources, and lower operating costs. Downscaling models, e.g., SDSM and LARS-WG, are frequently employed for downscaling current and future climate data and projections. The current research aims to evaluate the climate change impact on the drought phenomena in the Upper Zab River Basin in Northern Iraq while accounting for the uncertainty brought on by general circulation models (GCM) and scenarios for greenhouse gas emissions, which was done by likening the outcomes of a group of five GCM methods using the RCP4.5 and RCP8.5 scenarios and solely using recent periods [4]. The evaluation aims to investigate how Several researchers have explored the impact of climate change on arid and semiarid climates. They have examined the similarities and differences between these scenarios in terms of their ability to replicate dry climatic conditions. This study aims to assess the effects of climate change on water flow while considering the uncertainties associated with general circulation models (GCMs) and greenhouse gas emission scenarios. Specifically, it seeks to link the results of five GCM methods using the RCP4.5 and RCP8.5 scenarios and exclusively analyze recent time periods. [4]. The comparison seeks to investigate how similar and dissimilar these scenarios are in terms of their capacity to imitate climatic dryness. What would the variations and/or resemblances in assessing climate change's influence on climatic drought between the RCP4.5 and RCP8.5 scenarios utilizing near-future periods? This research can be considered as a beginning to address this subject.

2.MATERIALS AND METHODS

2.1.Data Collection and Analysis

The next set of data has been gathered:

(1) Between 1990/91 and 2021/22, daily weather information from thirteen gauging stations, including precipitation and maximum and minimum air temperatures, was collected. The research area's upper and lower sub-basins have several weather gauging with elevations extending from 233 to 1980 m.a.s.l. (Fig. 1 and Table 1). About 26,032 km² serves as a catchment area. The data was acquired from the Ministry of Agriculture and Water Resources in the Kurdistan Province of Iraq.

(2) Geographical information: The Global and Land Cover Facility [5] and the Global Administrative Areas Database provided the UZRB shape files and Iraqi boundaries [6], respectively.

The analysis listed below was completed:

(1) ArcGIS 10.3 software was used for the delineation of streamflow, Theissen network, basin boundary, and climatic gauging station position estimates.

(2) The Statistical Software for Social Sciences (SPSS) software was used to estimate adjustments and fill in data gaps for the study data sets for the daily climate, including tendency, monthly, and yearly quantities.

(3) The open-source Daniel's XL Toolbox Excel Add-In by downloading it from the following website: http://daniel-s-xl-toolbox.apps.informer.com/download. was used to convert charts created, creating graphics with precise dimensions and resolutions using Microsoft Excel software.

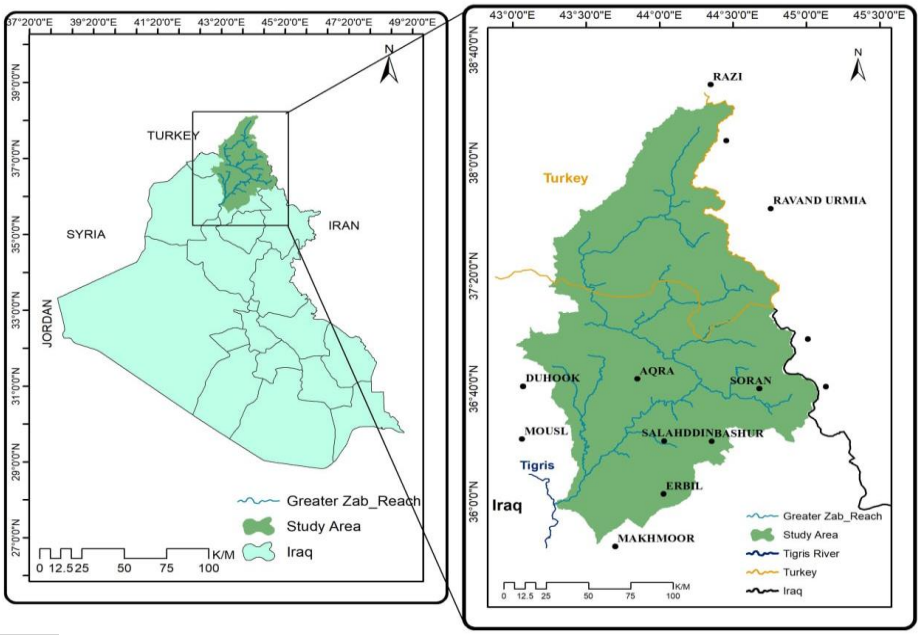

Fig. 1 The Hydrographic Scheme of the Upper Zab River Basin is Situated in Iraq.

Table 1 Situation of the Climate Places in the Greater Zab Basin, Northern Iraq, and Integration of the Fourth Assessment Report (AR5) of the Intergovernmental Panel on Climate Change (IPCC) into the Long Ashton Research Station Weather Generator (LARS-WG6).

Sub-basin	Station name	Latitude (°)	Longitude (°)	Altitude (m)	Length of Records
Upstream	Koozerash	38° 9' 0"	44° 27' 36"	1344	1990 – 2022
	Mirbad	36° 58' 48"	45° 0' 36"	1650	1990 – 2022
	Piranshahr	36° 42' 0"	45° 7' 48"	1350	1990 – 2022
	Ravand urmia	37° 45' 0"	44° 45' 36"	1290	1990 – 2022
	Soran	36° 41' 24"	44° 41' 24"	1154	1990 – 2022
	Razi	38° 28' 48"	44° 21' 0"	1980	1990 – 2022
Downstream	Aqra	36° 44' 24"	43° 52' 48"	505	1990 – 2022
	Bashur	36° 22' 12"	44° 22' 48"	977	1990 – 2022
	Duhook	36° 41' 24"	43° 7' 48"	436	1990 – 2022
	Erbil	36° 3' 36"	44° 3' 36"	439	1990 – 2022
	Makhmoor	35° 45' 0"	43° 45' 0"	306	1990 – 2022
	Mousl	36° 22' 12"	43° 7' 48"	233	1990 – 2022
	Salahddin	36° 22' 12"	44° 3' 36"	507	1990 – 2022
GCM Models	Organization				Spatial Resolution
CanESM2	Canadian Centre for Climate Modeling and Analysis, Canada				2.8◦ × 2.8◦
CSIRO-Mk3.6.0	Commonwealth Scientific and Industrial Research Organization, Australia				1.8◦ × 1.8◦
HadGEM2-ES	Met Office Hadley Center, United Kingdom				1.2◦ × 1.8◦
MIROC5	Atmosphere and Ocean Research Institute (The University of Tokyo), National Institute for Environmental Studies, and Japan Agency for Marine-Earth Science and Technology, Japan				1.4◦ × 1.4◦
NorESM1-M	Norwegian Climate Center, Norway				2.0◦ × 2.0◦

2.2.Basin Area Description

The Greater Zab River (GZR), the Tigris River's tributary, is a significant water source. The river starts in Turkey and flows across northern Iraq, as depicted in Fig. 1, before joining the Tigris River after around 372 km. The GZR and its streams are situated between longitudes 43° 18' 0" and 44° 18' 0 E and latitudes 36° 0' 0" and 38° 0' 0" N [7]. The approximate surface area of the GZR catchment (GZRC), which has an altitude range of 180–4000 m.a.s.l, is 26.331 km^2. Water erosion distributes sandstone, gravel, and conglomerates around the catchment. The GZR crosses several distinct climate and ecological zones. The river discharges 419 m^3/s on average and 1320 m^3/s at its highest, respectively [8]. The annual precipitation is between 350 and 1000 mm. The GZRC precipitation rates are usually the highest in the winter and spring. The precipitation respective percentages during the four seasons are around 48.9, 37.5, 12.9, and 0.7 percent. The GZRC stream system demonstrates substantial periodic stream fluctuations, with a peak flow in May and a low regular stream from July to December [8]. Irrigation Plans utilize several of the catchment's springs as sources. The World Energy Resources Forecast by the National Aeronautics and Space Administration (NASAPOWER) dataset served as the study's reliable substitute for using satellite data. The last 20 years' daily satellite data on temperature and rainfall (1990–2021) for each of the thirteen research locations are from (http://power.larc.nasa.gov) for the LARS-WG model calibration and validation procedure.

2.3.Drought Analysis

The reconnaissance drought index (RDI) has been extensively used for identifying, measuring, and observing droughts. The initial/alpha (RDI_k), normalized (RDI_n), and standardized (RDI_{st}) are three possible formulations of the RDI. While RDI_k can be used as an aridity index. RDI_{st} is frequently used to gauge how severe a drought is. The aggregated precipitation and potential evapotranspiration theories are the basic foundation for this index [9, 3]. Estimating RDI_{st} can be used to gauge how severe the drought is. This technique is popular, especially in arid and semiarid areas of the world [10].

To calculate the RDI_k, the following equation is generally employed [3]:

$$RDI_{\alpha_k^i} = \frac{\sum_{j=1}^{12} P_{ij}}{\sum_{j=1}^{12} PET_{ij}} \quad i=1 \text{ to } N \text{ and } j=1 \text{ to } 12 \qquad \textbf{(1)}$$

Let Pij and PETij represent the monthly precipitation (mm) and potential evapotranspiration (mm), respectively, for the jth month of the ith water year in Iraq. It is worth noting that the water year in Iraq commences in October. The climate data encompasses a total of N years, and the analyzed time step is denoted as K. For a range of time scales under consideration, the RDI_k values fit the gamma and the lognormal distributions in different places [9]. Eq. (2) can be applied to estimate RDI_{st} using the prior distribution [7]:

$$RDI_{st}^i = \frac{y_i - \bar{y}}{\hat{\sigma}_y} \qquad \textbf{(2)}$$

where $y_i = \ln(RDI_{\alpha ki})$, $\bar{y}$ is its arithmetic mean, and $\hat{\sigma}_y$ is the corresponding standard deviation. Compared to the research area's

typical climatic conditions, a positive value of RDI_{st} specifies a rainy time, while a negative figure denotes a dry time. Based on the RDI_{st} values, the intensity of the drought can be divided into eight classes, and it gets worse when the RDI_{st} numbers are low (Table 2). For a water year, RDI is estimated for reference periods of 1, 3, 6, 9, and 12 months. RDI is calculated for pre-established reference periods, suggesting that it has a varied quality compared to other drought indices.

Table 2 Drought Classification Based on Data from the Common Reconnaissance Drought Index (RDIst).

RDI_{st} value	Drought classes	
≥ 2.00	Extremely	
1.99 to 1.50	Severely	wet
1.49 to 1.00	Moderately	
0.99 to 0.00	Normal	-
0.00 to – 0.99	Near normal	
– 1.00 to – 1.49	Moderately	
– 1.50 to – 1.99	Severely	dry
≤ – 2.00	Extremely	

Because it is conceptually and practically simple and just relies on the proportion of yearly rainfall to potential evapotranspiration, RDI_{st} is intriguing. A categorization of environmental regions founded on aridity, stated as an index in which desert areas are grouped into various groups, was proposed by UNESCO in 1979 and is founded on the restricted values of RDI_{st},as revealed in Table 2.

2.4.Long Ashton Research Station Model

It was proven that it is successful in predicting climatological data at places for current and foreseeable climatic scenarios by applying the weather generator at the Long Ashton Research Station (LARS-WG6), which will be used related to the five GCMs (Table 1) to reduce uncertainty in climate projections and downscaling weather variables. The Coupled Model Intercomparison Project Phase 5 (CMIP5), collectively used in the IPCC Fifth Assessment Report, is incorporated into LARS-WG6. Only five of the nineteen models from the CMIP5 group were employed in this study, even though LARS-WG 6.0 offers them as part of its 19-model CMIP5 ensemble for climate prediction. Because of a lack of available computing and human resources, it is not practical to employ all the CMIP5 GCMs to project and analyze the effects of climate change [4]. Accordingly, five models were chosen based on research done in Iraq that was best adapted to forecasting future climate change [1,11]. Future precipitation and maximum temperature estimates were created for the study using LRS-WG. The LARS-WG6 uses the daily observed climate data from a particular place to compute various parameters for the likelihood ratios and relationships between meteorological variables. For additional information on the LARS-WG model's functionality, interested researchers can be referred to [4].

The LARS-WG modeling process is summarized in the stages below:

Two input files must contain the data that the model needs. The second is a site file containing information on each station's location, including CO2 levels, its name, and its location. The main file contains observed daily climate data for each station in the examined basin region. Before proceeding to the following step, these files were prepared and verified for each of the thirteen stations.

Analytical process: Once processed, three location variable files were created for every place using the observed data. The place data file is in the first file, "*.wgx." The third file, "*.tst," comprises the findings of statistical analyses that match the recorded data with the created data. Further statistics are listed in the second file, "*.stx."

Many statistical tests were considered to calibrate and validate the model. The daily distribution of maximum temperature and rainfall, as well as the comparison of the dry and wet series of seasonal distributions (DW_{Series}) and daily precipitation distributions ($D_{precipitation}$), which are computed from own scaled and recorded data, are all done using the Kolmogorov-Smirnov (K-S) statistical test.

This test allows researchers to check whether the two datasets are from the same distribution. The likelihood that predicted data would resemble real data is unknown when the p-value is modest, and the KS-value is large and should not be applied to model evaluation. According to [12], the acceptable interpretation threshold for the model results is set at a *p-value* of 0.01. The statistical analyses examine discrepancies between the produced and observed climate distributions.

The probability that both data sets are taken from the identical distribution is shown by the p-value each test provides, i.e., the parameter does not differ between the "real" and "fake" climates. Accordingly, an exceptionally low p-value implies that the generator is probably operating incorrectly, and the fake environment is unlikely to be identical to the climate that exists "really." If the *p-value* is exceedingly low, under the significance level, it is difficult for the created climate to match the real climate (set to 0.01 or 0.05). Since 0.05 is the typical significance level for statistical testing, a high *p-value* of 1.0 denotes a perfect match. A *p-value* of 1 indicates a perfect match; a *p-value* > 0.7 and 1 indicates a very excellent match; a *p-value* > 0.4 and 0.7 indicates a moderate match; and a *p-value* > 0.4 indicates a poor match. The variations between the recorded and modeled data could be significantly influenced by smoothing the recorded data by the model, random differences

in recorded data, errors in recorded data, and unusual weather phenomena at one of the regional weather stations in charge of severe climate occurrences during a given year.

3.ANALYSIS OF THE RESULTS

3.1.Calibrating and Verification of the Model's Accuracy

The calibration and validation of LARS-WG6 involved utilizing daily climate data for the baseline period from 1990 to 2021 across thirteen meteorological locations. The model's performance was assessed through mathematical tests and graphical comparisons. The Kolmogorov-Smirnov (K-S) test was employed to assess the equality of wet/dry series periodic distributions (WDSeries), daily rainfall distributions (RainD), daily minimum temperature distributions (TminD), and daily maximum temperature distributions (TmaxD) derived from both observed and downscaled data. To determine if two datasets may have originated from a similar distribution, the technique generates a "*p-value*" that affirms or rejects this, i.e., while there is an insignificant change between the recorded and the modeled weather for that parameter.

In the event that the generated weather exhibits a low p-value and a correspondingly high K-S value, indicating a significant deviation from real weather patterns, it should be disregarded. Although most statistics use a *p-value* of 0.05 as the significant threshold, it was proposed that a p-value of 0.01 can be used as an acceptable level of significance [13]. The main significant disparities between the recorded and simulated data arise from the LARAS-WG model's data smoothing, errors in the recorded data, random fluctuations in the recorded data, and extraordinary climate events that profoundly influence the weather of a specific year at a climate station. Using the downscaling simulation results in the impact analysis, a review of each month's daily rainfall distribution and the yearly variations in wet and dry spills were highly considered. Tables 3 and 4 exhibit the model performance in modeling the seasonal observed data and the daily rainfall every month, containing the K-S test outcomes from the validation stage. As demonstrated in Table 3, the wet/dry spells series fits the seasonal distribution exceptionally well, ranging from perfect to very good (1 > *p-value* 0.7).

Table 3 Results of the Kolmogorov-Smirnov (K-S) test for Seasons of Wet and Dry Years Series Distributions for a Baseline Period of 1990–2022 Long Ashton Research Station Weather Generator.

Sub-basin	Site name	Seasons for wet years							
		DJF[a]		MAM[b]		JJA[c]		SON[d]	
		K-S	*p*-value	K-S	*p*-value	K-S	*p*-value	K-S	*p*-value
US[e]	Koozerash	0.036	1.000[1]	0.062	1.000[1]	0.015	1.000[1]	0.016	1.000[1]
	Mirbad	0.015	1.000[1]	0.025	1.000[1]	0.098	1.000[1]	0.010	1.000[1]
	Piranshahr	0.056	1.000[1]	0.048	1.000[1]	0.000	1.000[1]	0.035	1.000[1]
	Ravand urmia	0.023	1.000[1]	0.065	1.000[1]	0.021	1.000[1]	0.071	1.000[1]
	Soran	0.025	1.000[1]	0.036	1.000[1]	0.087	1.000[1]	0.021	1.000[1]
	Razi	0.208	0.649[3]	0.025	1.000[1]	0.006	1.000[1]	0.015	1.000[1]
DS[f]	Aqra	0.219	0.584[3]	0.040	1.000[1]	0.087	1.000[1]	0.051	1.000[1]
	Bashur	0.040	1.000[1]	0.243	0.449	0.000	1.000[1]	0.064	1.000[1]
	Duhook	0.029	1.000[1]	0.045	1.000[1]	0.087	1.000[1]	0.022	1.000[1]
	Erbil	0.014	1.000[1]	0.200	0.697[3]	0.000	1.000[1]	0.141	0.964[2]
	Makhmoor	0.009	1.000[1]	0.065	1.000[1]	0.037	1.000[1]	0.055	1.000[1]
	Mousl	0.009	1.000[1]	0.024	1.000[1]	0.217	1.000[1]	0.062	1.000[1]
	Salahddin	0.037	1.000[1]	0.016	1.000[1]	0.131	0.982[2]	0.037	1.000[1]
Sub-basin	**Site name**	**Seasons for dry years**							
		DJF[a]		**MAM[b]**		**JJA[c]**		**SON[d]**	
		K-S	***p*-value**	**K-S**	***p*-value**	**K-S**	***p*-value**	**K-S**	***p*-value**
US[e]	Koozerash	0.046	1.000[1]	0.113	0.997[2]	0.093	1.000[1]	0.078	1.000[1]
	Mirbad	0.038	1.000[1]	0.076	1.000[1]	0.061	1.000[1]	0.060	1.000[1]
	Piranshahr	0.135	0.976[2]	0.087	1.000[1]	0.174	0.842[2]	0.095	1.000[1]
	Ravand urmia	0.066	1.000[1]	0.036	1.000[1]	0.138	0.971[2]	0.053	1.000[1]
	Soran	0.058	1.000[1]	0.057	1.000[1]	0.087	1.000[1]	0.059	1.000[1]
	Razi	0.072	1.000[1]	0.103	0.999[2]	0.099	1.000[1]	0.100	1.000[1]
DS[f]	Aqra	0.047	1.000[1]	0.088	1.000[1]	0.130	0.984[2]	0.145	0.954[2]
	Bashur	0.091	1.000[1]	0.065	1.000[1]	0.131	0.982[2]	0.089	1.000[1]
	Duhook	0.046	1.000[1]	0.067	1.000[1]	0.218	0.589[3]	0.091	1.000[1]
	Erbil	0.091	1.000[1]	0.070	1.000[1]	0.305	0.193[4]	0.087	1.000[1]
	Makhmoor	0.052	1.000[1]	0.073	1.000[1]	0.066	1.000[1]	0.054	1.000[1]
	Mousl	0.067	1.000[1]	0.086	1.000[1]	0.305	0.193[4]	0.054	1.000[1]
	Salahddin	0.049	1.000[1]	0.061	1.000[1]	0.131	0.982[2]	0.067	1.000[1]

[a]Winter season (Dec, Jan, and Feb); [b]Spring season (Mar, Apr, and May); [c]Summer season (Jun, Jul, and Aug); [d]Autumn season (Sep, Oct, and Nov); [e]Upstream; [f]Downstream; [1]Perfect fit (*p*-value = 1); [2]Very good fit (1 > *p*-value ≥ 0.7); [3]Good fit (0.7 > *p*-value ≥ 0.4); [4]Poor fit (0.4 > *p*-value).

LARAS-WG6 demonstrates a highly favorable evaluation, ranging from very good (with a p-value greater than 0.7) to perfect (with a p-value between 0.7 and 1), in terms of its ability to accurately replicate the wet/dry period series distributions specifically for the spring season (March, April, and May). However, the summer "JJA" season (June, July, and August) showed slight variations in the weather generator's performance. The wet spell distribution in many stations is only fit by the model fairly (0.7 > *p-value* 0.4) to poorly (0.4 > *p-value*), even though it fits the dry spell distribution in the winter "DJF" flawlessly. The dry JJA season was regarded as the cause of this poor outcome. As there was little to no rainfall this season, the model would perform poorly because it would be unable to include any rainy spells. In addition, as shown in Table 4, except for the summer, LARS-performance WG6 in simulating daily rain distributions ranges from very good to perfect. This summer performance issue can be attributed to a similar cause as the presentation issue with the simulation of cyclical distributions that was earlier noted.

Table 4 The Long Ashton Research Station Weather Generator Validation Results for Daily Rain Distributions Throughout the Baseline Period of 1990–2022, Including the Kolmogorov–Smirnov (K–S) test.

Sub-basin	Site Name	January		February		March		April	
		K-S	*p-value*	K-S	*p-value*	K-S	*p-value*	K-S	*p-value*
Upstream	Koozerash	0.071	1.000[1]	0.083	1.000[1]	0.064	1.000[1]	0.063	1.000[1]
	Mirbad	0.065	1.000[1]	0.065	1.000[1]	0.071	1.000[1]	0.069	1.000[1]
	Piranshahr	0.130	0.984[2]	0.065	1.000[1]	0.065	1.000[1]	0.132	0.981[2]
	Ravand urmia	0.130	0.984[2]	0.063	1.000[1]	0.065	1.000[1]	0.061	1.000[1]
	Soran	0.130	0.984[2]	0.136	0.974[2]	0.065	1.000[1]	0.064	1.000[1]
	Razi	0.062	1.000[1]	0.065	1.000[1]	0.079	1.000[1]	0.064	1.000[1]
Downstream	Aqra	0.065	1.000[1]	0.130	0.984[2]	0.065	1.000[1]	0.064	1.000[1]
	Bashur	0.065	1.000[1]	0.068	1.000[1]	0.065	1.000[1]	0.064	1.000[1]
	Duhook	0.065	1.000[1]	0.130	0.984[2]	0.065	1.000[1]	0.064	1.000[1]
	Erbil	0.065	1.000[1]	0.130	0.984[2]	0.065	1.000[1]	0.070	1.000[1]
	Makhmoor	0.073	1.000[1]	0.059	1.000[1]	0.077	1.000[1]	0.068	1.000[1]
	Mousl	0.116	0.996[2]	0.130	0.984[2]	0.065	1.000[1]	0.063	1.000[1]
	Salahddin	0.130	0.984[2]	0.065	1.000[1]	0.130	0.984[2]	0.064	1.000[1]
Sub-basin	**Site Name**	**May**		**June**		**July**		**August**	
		K-S	*p-value*	K-S	*p-value*	K-S	*p-value*	K-S	*p-value*
Upstream	Koozerash	0.069	1.000[1]	0.127	0.987[2]	0.200	0.697[3]	0.087	1.000[1]
	Mirbad	0.077	1.000[1]	0.065	1.000[1]	0.080	1.000[1]	0.131	0.982[2]
	Piranshahr	0.141	0.964[2]	0.261	0.359[4]	0.391	0.043[4]	1.000	0.000[4]
	Ravand urmia	0.136	0.974[2]	0.190	0.755[2]	0.174	0.842[2]	0.261	0.359[4]
	Soran	0.065	1.000[1]	0.392	0.042[4]	0.652	0.000[4]	(-)*	(-)*
	Razi	0.066	1.000[1]	0.110	0.998[2]	0.130	0.984[2]	0.066	1.000[1]
Downstream	Aqra	0.064	1.000[1]	0.652	0.000[4]	1.000	0.000[4]	0.652	0.000[4]
	Bashur	0.134	0.978[2]	0.158	0.913[4]	(-)*	(-)*	(-)*	(-)*
	Duhook	0.063	1.000[1]	0.218	0.589[3]	(-)*	(-)*	1.000	0.000[4]
	Erbil	0.072	1.000[1]	0.217	0.595[3]	(-)*	(-)*	(-)*	(-)*
	Makhmoor	0.070	1.000[1]	0.073	1.000[1]	0.064	1.000[1]	0.123	0.991[2]
	Mousl	0.065	1.000[1]	0.305	0.193[4]	(-)*	(-)*	(-)*	(-)*
	Salahddin	0.063	1.000[1]	0.261	0.359[4]	(-)*	(-)*	(-)*	(-)*
Sub-basin	**Site Name**	**September**		**October**		**November**		**December**	
		K-S	*p-value*	K-S	*p-value*	K-S	*p-value*	K-S	*p-value*
Upstream	Koozerash	0.067	1.000[1]	0.064	1.000[1]	0.063	1.000[1]	0.068	1.000[1]
	Mirbad	0.177	0.826[2]	0.079	1.000[1]	0.064	1.000[1]	0.080	1.000[1]
	Piranshahr	0.304	0.196[4]	0.083	1.000[1]	0.066	1.000[1]	0.145	0.954[2]
	Ravand urmia	0.140	0.966[2]	0.070	1.000[1]	0.072	1.000[1]	0.126	0.988[2]
	Soran	0.072	1.000[1]	0.071	1.000[1]	0.066	1.000[1]	0.064	1.000[1]
	Razi	0.065	1.000[1]	0.128	0.986[2]	0.064	1.000[1]	0.141	0.964[2]
Downstream	Aqra	0.217	0.595[3]	0.127	0.987[2]	0.075	1.000[1]	0.126	0.988[2]
	Bashur	0.174	0.842[2]	0.173	0.847[2]	0.198	0.709[2]	0.124	0.990[2]
	Duhook	0.348	0.096[4]	0.082	1.000[1]	0.198	0.709[2]	0.063	1.000[1]
	Erbil	0.870	0.000[4]	0.089	1.000[1]	0.175	0.837[2]	0.063	1.000[1]
	Makhmoor	0.150	0.940[2]	0.081	1.000[1]	0.064	1.000[1]	0.128	0.986[2]
	Mousl	0.391	0.043[4]	0.123	0.991[2]	0.128	0.986[2]	0.062	1.000[1]
	Salahddin	0.217	0.595[3]	0.164	0.888[2]	0.127	0.987[2]	0.140	0.966[2]

Below the detected limit; [1]Perfect fit (*p-value* = 1); [2]Very good fit (1 > *p-value* ≥ 0.7); [3]Good fit (0.7 > *p-value* ≥ 0.4); and [4]Poor fit (0.4 > *p-value*).

To enhance the level of confidence in the predictive capability of the model, a comprehensive analysis was conducted by comparing the monthly averages and standard deviations (SD) of observed and simulated rainfall across all stations. This comparison aimed to evaluate the model's accuracy and reliability in replicating rainfall patterns. Fig. 3 demonstrates how effectively LARS-WG6 simulated T_{max} and T_{min} monthly mean values, demonstrating that this iteration of LARS-WG can accurately forecast extreme air temperatures. The model excellently provides daily precipitation, i.e., T_{min} and T_{max} in the

basin. Hence, subjected to the five groups of GCM and SRA2 scenario, daily climatic data forecasting is a possibility for the basin for the future 2021–2040.

4.DISCUSSION

Each hydro-climatic study must include rainfall as a necessary component. Unfortunately, there is a lack of long-term accurate precipitation data in many developing nations [14-17], particularly in places with active conflicts. The climate in Iraq, which has a land area of 438,320 km², varies significantly from the Mediterranean in the north and northeast to continental semiarid and arid in the south. As a result, investigations on Iraq's climate or hydrology need widely disseminated accurate precipitation data. Precipitation is not, however, accurately measured in the country. There are just limited long-term precipitation records. No precipitation gauge has been constructed in the country since the 1980s due to the political unrest and conflicts.

4.1.Estimation of the Weather Variables'

Using RCP8.5 and RCP4.5, two important emission scenarios created by the five designated GCMs, the weather generator model will work well in the future (2021– 2040), depending on the calibration procedure and validation study findings. For the US and DS sub-basins, the T_{max} and rainfall were downscaled using the output from the GCM models MIROC5, CSIRO-MK3.6.0, CanESM2, HadGEM2-ES, and NorESM1-M. Figs. 3 and 4 display predicted temperatures and precipitation, respectively. The range of five selected GCMs is shown in Fig. 3, along with the mean monthly T_{max} for future times. Plots of the mean monthly T_{max} across the US and DS local sub-basins revealed that the summer months (July and August) had the most significant rises, whereas the winter months (Dec. and Jan.) had the minimum rises. Between the observed and anticipated RCP scenarios, the graphs likewise show a steady drop in T_{max}. HadGEM2-ES reported at the DS sub-basin in July that the T_{max} predicted by the model by RCP8.5 (about 44.5°C). Fig. 3 displays the annual average expected T_{max} difference from the observation time for each of the five GCM models considered in this study. According to the results, the average annual T_{max} under RCP4.5 dropped to 6.20 and 5.78 °C for the US and DS sub-basins, respectively. Under RCP8.5, the temperature reduction ranged from 6.10 to 5.58 °C for the US and DS sub-basins, respectively. Even though global warming has not been uniform, the rising trend in the average global temperature indicates that more regions are warming rather than cooling. The total land and ocean temperature has risen at an average rate of 0.08 °C every decade since 1880, according to NOAA's 2021 Annual Climate Report [18]. However, the average growth rate since 1981 has been more than twice as fast: 0.18 °C per decade. Temperature measurement statistics showed that Iraq's annual average temperature has climbed by 0.7 °C per century since the 1990s; however, this number increased from 21.87 °C to 21.13 °C during 1990-2020 [19].

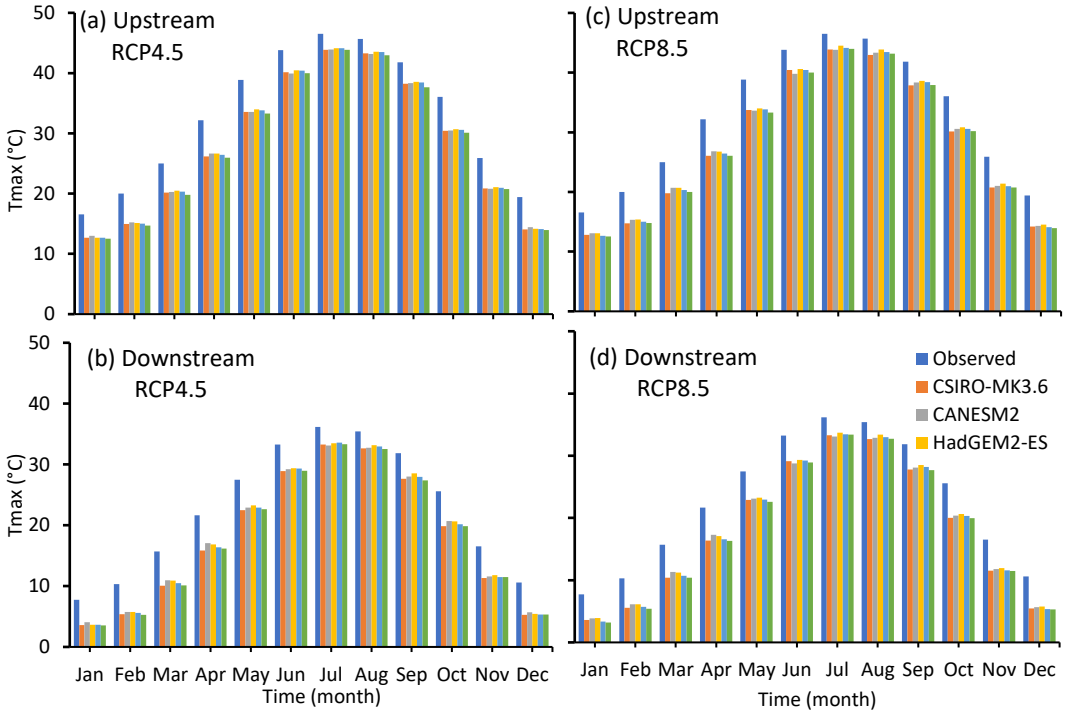

Fig. 3 Comparison of Observed Average Monthly Maximum Temperatures for the Period (1990–2021) with those Predicted by the RCP4.5 and RCP8.5 Scenarios Using Five GCMs (2021–2040).

4.2.Precipitation Predictions

The precipitation forecasts for the two RCP4.5 and RCP8.5 scenarios are displayed in Fig. 4, showing that the upstream and downstream sub-basins of the five selected GCMs have different predicted values of precipitation because there were days with no data since precipitation does not occur continuously throughout the year. Therefore, it is difficult to anticipate future precipitation. This graph demonstrates that for each of the five selected GCMs across the selected future period, there are different forecast trends. Because each GCM model could produce a different projection, these variations showed the challenges and related uncertainty in forecasting rainfall values using a single GCM model. In contrast to other models like NorESM1-M and MIROC5, the CANESM2 model predicted increased precipitation between the two sub-basins in various seasons, with the total changing depending on the PCR 8.5. Other models, like NorESM1-M and MIROC5, predicted a minor reduction or rise in precipitation or that there would not be any appreciable rainfall variation in the future. The upstream sub-basin experienced the most significant increase in precipitation (14.10 mm), according to the CanESM2 model, in the winter (DJF) season. The MIROC5 model during winter (DJF) at the upstream sub-basin produced the most significant decrease in rainfall (9.44 mm). The findings align with climate change studies in Iraq and other surrounding countries [1, 11], which show that this region in northern Iraq is experiencing an altered trend of variations in rainfall [1, 3, 11].

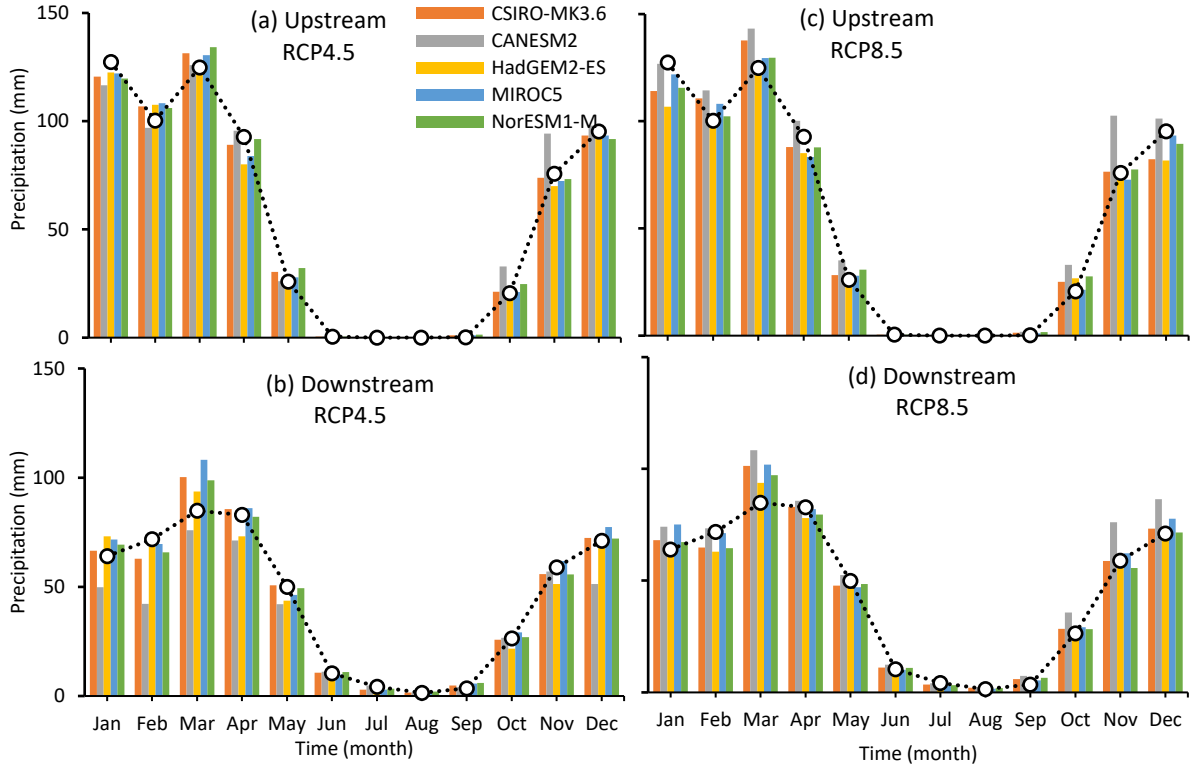

Fig. 4 Comparison of the Monthly Mean Precipitation Values Observed (1990–2022) and the Projected by Scenarios (RCP4.5) and (RCP8.5) Applying Five General Circulation Models (GCM) for the Years (2021–2040) in the Upstream and Downstream Greater Zab Sub-Basins.

4.3.Variation of Drought

The selected case study focuses on semiarid regions, with a particular emphasis on areas that are highly vulnerable to the effects of climate change. According to Fig. 5 Currently, the DS sub-basin is classified as experiencing near-normal to moderately dry conditions, while the US sub-basin is classified as having a combination of severely wet and moderately wet to normal conditions. However, over the following twenty years, they are predicted to change from extremely moderately wet to moderately dry and from moderately wet to severely dry, respectively. The temporal evolution of the RDI_{st} index for UZB from 1990 to 2021 and from 2022 to 2040 is depicted in Fig. 5. The findings revealed an inconsistent cycle of dry and wet periods throughout the research period. The hydrological years 1999–2000 and 2007–2008 experienced droughts, although there were some variances between the US and the DS sub-basins. Droughts usually start at the beginning of the rainy season because of a delay in or a reduction in rainfall. The DS sub-basin experienced the worst levels of drought, with average RDI_{st} values of -1.97 and -1.64, respectively, in the years 1999–2000 and 2007–2008. In addition, moderate to severe droughts with average RDI_{st} values of -0.81 and -1.84, respectively, also affected the

US sub-basin stations in 1999–2000 and 2007–2008. The temporal evolution of the RDI_{st} index for UZB from 1990 to 2021 and from 2022 to 2040 is depicted in Fig. 5. In addition, the US sub-basin stations also experienced moderate to severe droughts in 1999–2000 and 2007–2008, with average RDI_{st} values of -0.81 and -1.84, respectively.

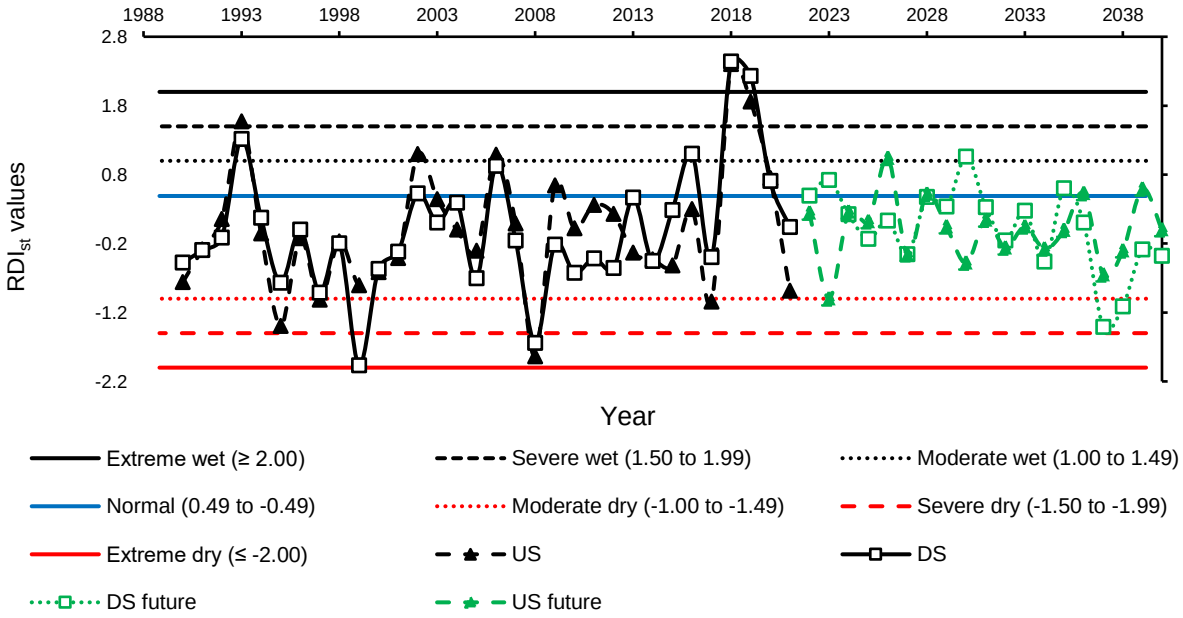

Fig. 5 Temporal Variation of the Annual Values of the Standardized Reconnaissance Drought Index (RDIst) Estimated (1990–2021) and the Projected by Scenarios (RCP4.5) and (RCP8.5) Using Five General Circulation Models (GCM) for the Period (2021–2040) in the Upstream and Downstream Greater Zab Sub-Basins.

5.CONCLUSIONS

The Weather Generator model's propensity to forecast daily rainfall and T_{max} was examined in this study. The northern Iraqi region was then utilized to explore the effects of climate change by projecting future precipitation and temperature variations, which was founded on the outcomes of five GCMs for the three-time period of the RCP 4.5 and RCP 8.5 scenarios (2021–2040). Using data from the baseline period, 1990–2020, three selected stations in the study area were used for calibration and validation testing. The investigation concluded that the model LARSWG performs effectively when downscaling daily temperature and precipitation for all studied sites. The findings indicated that the T_{max} is predicted to increase by 2.27 to 3.71 °C at the US and the DS research sub-basin locations for the three future periods under both RCP scenarios. For each study meteorological station, the downscaled rainfall from the five GCMs models exhibits various outlines for the selected period. Under RCP8.5, the CanESM2 Model anticipated the highest precipitation increase (14.10 mm) at the US sub-basin, while the MIROC5 Model forecasted the highest precipitation decrease (9.44 mm) at the US sub-basin.

REFRENCES

[1] Mohammed ZM , Hassan WH. **Climate Change and the Projection of Future Temperature and Precipitation in Southern Iraq Using a LARS-WG Model**. *Modeling Earth Systems and Environment* 2022; **8**(3):4205–4218.

[2] Archer D, Rahmstorf S. **The Climate Crisis: An Introductory Guide to Climate Change.** 4th ed., Cambridge: Choice Reviews Online; 2010.

[3] Mohammed R, Scholz M. **Climate Change and Water Resources in Arid Regions: Uncertainty of the Baseline Time Period**. *Water Resources Management* 2019; **33**(15): 5015-5033.

[4] Semenov MA , Stratonovitch P. **Use of Multi-Model Ensembles from Global Climate Models for Assessment of Climate Change Impacts**. *Climate Research* 2010; **41**(1): 1–14.

[5] Herrmann H, Bucksch H. **Dictionary Geotechnical Engineering/ Wörterbuch GeoTechnik : English-German / Englisch - Deutsch**. 2nd ed., Berlin, Heidelberg : Springer Berlin Heidelberg; 2014.

[6] Robert J. Hijmans. Global Administrative Areas (GADM) | Geospatial Centre | University of Waterloo. 2012

https://uwaterloo.ca/library/geospatial/collections/us-and-world-geospatial-data-resources/global-administrative-areas-gadm (12 July 2023, date last accessed).

[7] Mohammed R, Scholz M .**Climate Variability Impact on the Spatiotemporal Characteristics of Drought and Aridityin Arid and Semi-Arid Regions**. *Water Resources Management* 2019; **33**(15): 5015–5033.

[8] UN-ESCWA. **Inventory of Shared Water Resources in Western Asia.** Salim Dabbous Printing Company: Beirut; 2013, pp. 1-626.

[9] Tsakiris G, Pangalou D, Vangelis H. **Regional Drought Assessment Based on the Reconnaissance Drought Index (RDI)**. *Water Resources Management* 2007; **21**(5): 821–833.

[10] Vangelis H, Tigkas D, Tsakiris G . **The Effect of PET Method on Reconnaissance Drought Index (RDI) Calculation**. *Journal of Arid Environments* 2013; **88**: 130–140.

[11] Khalaf RM, Hussein HH, Hassan WH, Mohammed ZM, Nile BK . **Projections of Precipitation and Temperature in Southern Iraq Using a LARS-WG Stochastic Weather Generator**. *Physics and Chemistry of the Earth* 2022; **128**: 103224.

[12] Semenov M A, Barrow, E M. **Use of a Stochastic Weather Generator in the Development of Climate Change Scenarios**. *Climatic Change* 1997; **35**(4) :397–414.

[13] Semenov M A , Pilkington-Bennett S, Calanca P. **Validation of ELPIS 1980-2010 Baseline Scenarios Using the Observed European Climate Assessment Data Set**. *Climate Research* 2013; **57**(1): 1–9.

[14] Flato G, Marotzke J, Abiodun B, Braconnot P, Chou SC, Collins W, Rummukainen M. **Evaluation of Climate Models.** In: Stocker TF, Qin D, Plattner GK, Tignor M, Allen S, Boschung J, et al. (Eds.), Climate Change 2013: The Physical Science Basis. Contribution of Working Group I to the Fifth Assessment Report of the Intergovernmental Panel on Climate Change (pp. 741-866). Cambridge: Cambridge University Press.

[15] Nkiaka E, Nawaz R, Lovett JC. **Assessing the Reliability and Uncertainties of Projected Changes in Precipitation and Temperature in Coupled Model Intercomparison Project Phase 5 Models Over the Lake Chad Basin.** *International Journal of Climatology* 2018; **38**(14):5136-5152.

[16] Agha OM. **Investigating the Meteorological Drought Using CZI in Nineveh Governorate, Iraq**. *Tikrit Journal of Engineering Sciences* 2021; **28**(4):14-24.

[17] Awchi TA, Jasim AI. **Rainfall Data Analysis and Study of Meteorological Draught in Iraq for the Period 1970-2010**. *Tikrit Journal of Engineering Sciences* 2017; **24**(1):110-121.

[18] Internet Source: Global Climate Report. National Centers for Environmental Information (NCEI). 2022: Available from: https://www.ncei.noaa.gov/access/monitoring/monthly-report/global/2022 (30 September 2023, date last accessed).

[19] Al-Maliki L A, Al-Mamoori S K, Al-Ansari N, El-Tawel K, Comair F G. **Climate Change Impact on Water Resources of Iraq (a Review of Literature).** *IOP Conference: Series Earth and Environmental Science* 2022; **1120**(1): 012025, (1-15).